Separation of Auger transitions into different repulsive states after *K*-shell photoionization of N₂ molecules

N. A. Cherepkov,[1,2] S. K. Semenov,[1] M. S. Schöffler,[2] J. Titze,[2] N. Petridis,[2] T. Jahnke,[2] K. Cole,[2] L. Ph. H. Schmidt,[2]
A. Czasch,[2] D. Akoury,[2,3] O. Jagutzki,[2] J. B. Williams,[4] C. L. Cocke,[5] T. Osipov,[3] S. Lee,[3] M. H. Prior,[3] A. Belkacem,[3]
A. L. Landers,[4] H. Schmidt-Böcking,[2] Th. Weber,[3] and R. Dörner[2]

[1]*State University of Aerospace Instrumentation, 190000 St. Petersburg, Russia*
[2]*Institut für Kernphysik, University Frankfurt, Max-von-Laue-Str. 1, D-60438 Frankfurt, Germany*
[3]*Lawrence Berkeley National Laboratory, Berkeley, California 94720, USA*
[4]*Department of Physics, Auburn University, Auburn, Alabama 36849, USA*
[5]*Department of Physics, Kansas State University, Cardwell Hall, Manhattan, Kansas 66506, USA*
(Received 20 August 2009; published 24 November 2009)

The Auger transitions to different repulsive doubly charged molecular ion states are separated by measuring the angular resolved photoelectrons and Auger electrons in coincidence in the molecular fixed frame. The separation is achieved by comparing the experimental Auger-electron angular distributions at different kinetic-energy release values with theoretical curves calculated for different final dicationic states.

Auger-electron spectroscopy for a long time was used as a powerful technique for probing orbital and band structure of valence and core levels in atoms, molecules, clusters, solids, surfaces, and adsorbates. In atoms the Auger decay corresponds to a transition between two (quasi)discrete states, therefore main attention in the atomic Auger-electron spectroscopy studies was focused on the identification of discrete lines. As compared to atoms, in molecules nuclear motion introduces a new degree of freedom which enters into the energy balance. This substantially modifies the molecular Auger-electron spectra. First, the discrete lines acquire the vibrational splitting which usually is of the same order of magnitude as the line widths. In addition, the photoionization followed by Auger decay produces a doubly charged molecular ion which often dissociates creating atomic ions. For this a part of the Auger transition energy needs to be transferred to the nuclear motion, and instead of a well defined discrete line in the electron spectrum a broad continuum appears. This continuum cannot be identified by its energy position since transition to several repulsive final states can contribute at the same Auger-electron energy. Therefore a basically new method is needed for studying the continuous Auger-electron emission in molecules.

In this Rapid Communication we study the processes initiated by photoionization of the *K*-shell of N₂ molecule. The photoionization produces highly excited molecular ion state which decays, according to the linewidth, within a short time of about 7 fs, predominantly by emission of a fast Auger electron (around 365 eV). As a result, a doubly charged molecular ion is created with two holes in valence shells. At the next step this doubly charged ion dissociates mainly into two N^+ atomic ions with the kinetic-energy release (KER) in the region of 4 to 20 eV. The dissociation time is usually short compared to the molecular rotation, therefore the direction of motion of the atomic ions gives the direction of the molecular axis at the time of the photoabsorption and the Auger decay.

The Auger decay of core ionized N₂ molecules has been studied by many different methods including the Auger-electron spectroscopy [1,2], KER spectroscopy of the two N^+ ions [3]. In these studies, like in studies of atomic Auger decay, mainly the narrow line structure in the energy spectra have been investigated. We report on the most detailed study of the molecular Auger decay process by detecting the photoelectron, the Auger electron and the two atomic singly charged ions in coincidence (all of them being energy and angular resolved) using the the cold target recoil ion momentum spectroscopy (COLTRIMS) technique [4–8]. The *K* shell of N₂ molecule due to symmetry requirements is split into two states, $1\sigma_g$ and $1\sigma_u$, therefore it is of great importance to separate the Auger decay processes of these two hole states. Their energy splitting is rather small, about 100 meV, which is nearly equal to the width of these states which amounts to 120 meV [9–11]. Since the Auger spectrum is mostly continuous, the hole states cannot be resolved from the Auger-electron spectrum. However, $1\sigma_g$ and $1\sigma_u$ states of N₂ have been resolved recently in Refs. [9–11]. by a very high-resolution measurement of the photoelectron line shape. That high resolution is yet unattainable in a coincidence experiment like ours, therefore one must look for another method to resolve the $1\sigma_g$ and $1\sigma_u$ states.

From calculations of the photoelectron angular distributions it is known that at some ejection angles predominantly $1\sigma_g$ or $1\sigma_u$ shell is contributing [4,5]. Figure 1 shows the theoretical angular distribution of photoelectrons in the molecular frame ejected by circularly polarized light at photon energy 419 eV corresponding to the well-known σ^* shape resonance in the photoabsorption cross section [12]. It is seen that at the angles of 215–265° the predominant contribution is given by the photoelectrons ejected from $1\sigma_g$ shell (dashed arrow in Fig. 1). At the angles of 115–150°, vice versa, the predominant contribution is given by the $1\sigma_u$ (solid arrow in Fig. 1). Thus by measuring the Auger-electron angular distribution in coincidence with the photoelectrons collected at the angles mentioned above one can separate the contributions of the Auger decay with original vacancies in the $1\sigma_g$ and $1\sigma_u$ shells without need to resolve these transitions in energy [5]. Under these conditions to a
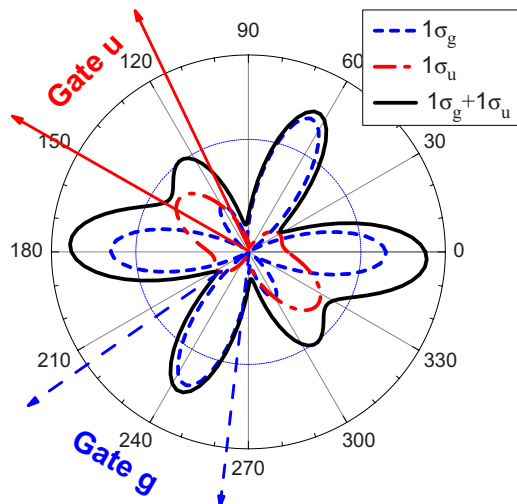
FIG. 1. (Color online) Molecular frame photoelectron angular distributions calculated for absorption of left handed circularly polarized light of energy 419 eV. The molecular axis is parallel to the horizontal axis. The contributions of $1\sigma_g$ and $1\sigma_u$ hole states are shown by dot-dashed (red) and dashed (blue) lines, respectively. Their sum is shown by solid line (black).

good approximation, the photoionization and the Auger decay processes can be treated independently in the framework of the two-step model [5]. Our calculations show that the Auger-electron angular distributions for the $1\sigma_g$ and $1\sigma_u$ shells are strongly different. While comparing experimental and theoretical angular distributions, one can identify transitions into different final dicationic states even though they completely overlap in Auger-electron energy. It is important that method makes possible study of the continuous part of the Auger-electron spectrum. This is difficult to do by other methods [13,14]. This continuum is formed by Auger transitions into repulsive doubly charged molecular ion states which do not create any resonance structure. However, the most intense resonant Auger transitions can also be studied by this method.

The experiment was performed at beamline 11.0.2 of the Advanced Light Source of Lawrence Berkeley Laboratory via the COLTRIMS technique [6–8]. The circularly polarized photon beam at 419 eV is crossed with a supersonic molecular beam of N_2 in the vibrational ground state. Electrons created in the interaction region (0.1 mm^3) were guided by parallel electric (12 V/cm) and magnetic (6.5 G) fields toward a multichannel plate detector (diameter 80 mm) with delay-line position readout [15,16]. This yielded 4π collection solid angle for the photoelectrons of about 10 eV. Opposite to the electron detector a second detector for the ions was placed 76cm away from the interaction point. This ion arm of the spectrometer collected ions that fragmented within 15° parallel to the electric-field axis of our spectrometer. We detected both ions in coincidence. An electrostatic lens and a field free drift tube was placed in the ion flight path to focus ions starting at different position within the reaction zone to the same time of flight and same position on the detector (see Fig. 12 in [6]). For the ions and the photoelectron the final-state momenta are calculated from the mea-

sured times of flight and positions of impact on the detectors. While the long ion arm sacrifices collection solid angle for the ions, it allows for sufficient momentum resolution on the center-of-mass momentum of the two ions to resolve the recoil momentum imparted by the Auger and photoelectron onto the center of mass. Hence the Auger electron was not detected directly but its momentum was inferred from the measured momenta of the photoelectron and both ions while using momentum conservation. Therefore the effective solid angle for the Auger electron was 4π. We obtained an overall resolution of better than 50 meV for the KER and 0.5 atomic unit momentum resolution of the center-of-mass motion (the calculated Auger electron).

Our calculations have been performed in prolate spheroidal coordinates as it was described earlier in [17]. The two steps (the photoionization and the Auger decay) are treated in the following way. At first the single electron wave functions of the ground state of the neutral molecule are calculated in the Hartree-Fock (HF) approximation. The photoelectron wave function is found in the relaxed core HF (RCHF) approximation with the fractional charge 0.7 instead of 1 as was proposed in [18] for a better description of the core relaxation effect. It is orthogonalized to the ground-state wave functions. With these wave functions the dipole matrix elements are calculated. Many-electron correlations are taken into account in the random-phase approximation as was described in [17].

The initial state for the Auger decay is described by the same self-consistent HF wave functions of the singly charged molecular ion, $\varphi_j^{(i)}(\mathbf{r})$, as in the photoionization step. For the doubly charged final molecular ion state another set of the self-consistent HF wave functions $\varphi_j^{(f)}(\mathbf{r})$ is calculated. The Auger-electron wave function is calculated in the frozen field of the doubly charged ion with the same internuclear distance as in the ground state. The Auger decay amplitude is described by the Coulomb matrix element containing the wave functions $\varphi_j^{(i)}(\mathbf{r})$ and $\varphi_j^{(f)}(\mathbf{r})$ which are not orthogonal. Therefore we calculate also the overlap matrix between the HF orbitals of the initial and final states $\mathbf{S}_{jk}=\langle \varphi_j^{(f)}|\varphi_k^{(i)}\rangle$ and obtain the Auger amplitude following the procedure proposed in [19]. The Auger-electron energy in the particular cases considered here is large, about 350 eV, therefore the contribution of many-electron correlations is expected to be small, and we restricted calculations by the HF approximation as it was done in [20].

Figure 2 shows the angular distributions of the Auger electrons for photon energy 419 eV measured in coincidence with the photoelectrons ejected at two fixed directions corresponding to ionization of one of the K shells as shown in Fig. 1. In this way the Auger decay processes of the $1\sigma_g$ and $1\sigma_u$ hole states are separated and are shown in Figs. 2(a) and 2(b), respectively. The vertical axis in these figures is the KER. One can single out three regions corresponding to KER values 6.8–7.5, 7.5–9.5, and 10.3–11.5 eV, where the angular distributions have different characteristic features. To interpret these spectra, we performed calculations of Auger-electron angular distributions for all possible doubly charged molecular ion states with two holes in the outermost $3\sigma_g$, $1\pi_u$, or $2\sigma_u$ shells. These angular distributions strongly depend on the dicationic final state, and by comparison with the
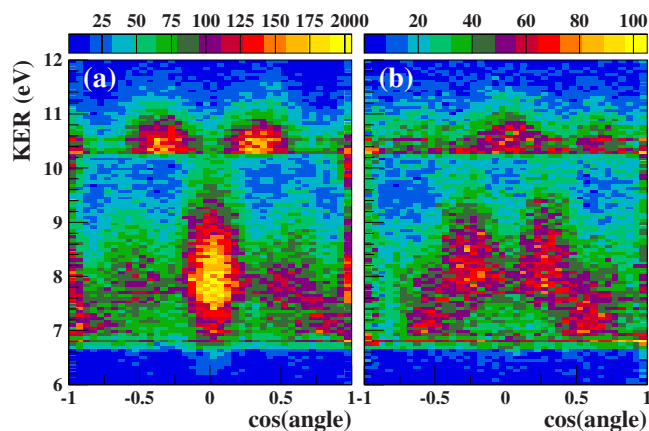
FIG. 2. (Color online) Auger-electron intensities as a function of cos of the ejection angle θ relative to the molecular axis (horizontal axis) and of the KER (vertical axis). (a) and (b) correspond to the Auger decay of $1\sigma_g$ and $1\sigma_u$ hole states, respectively, selected via the gates on the photoelectron angle as marked in Fig. 1.

FIG. 4. (Color online) Potential-energy curves from Refs. [3,24]. (solid lines) and from [25] (dot-dashed line), and our total KER spectrum (in arbitrary units). The zero KER energy corresponds to the dissociation limit into the $N^+(^3P) + N^+(^3P)$ ion states. The shaded areas correspond to the contributions of three different dicationic states mentioned in the figure.

experiment one can unambiguously determine the main Auger decay channels contributing at a given KER value. As an example, we show in Fig. 3 the comparison of calculated and measured Auger-electron angular distributions at KER values from 8 to 9 eV. For a qualitative description of the experimental data it was sufficient to include the contributions of only two transitions to the doubly charged molecular ion states $(1\pi_u)^{-2}$ $^1\Delta_g$ and $(1\pi_u)^{-2}$ $^1\Sigma_g^+$. The $(1\pi_u)^{-2}$ $^1\Delta_g$ state is responsible for the intensive lobe at the ejection angle 90° (above the horizontal axis) and two smaller lobes at 57.5 and 122.5° for the $1\sigma_g$ state, and for the intensive lobes at the angles 75 and 105° for the $1\sigma_u$ state. The $(1\pi_u)^{-2}$ $^1\Sigma_g^+$ state contributes mainly along the molecular axis at the angles 0 and 180° (qualitatively similar results though without resolving the contributions of $1\sigma_g$ and $1\sigma_u$ hole states have been obtained theoretically in [13]). There are two theoretical curves in Fig. 3. Dot-dashed lines show the results obtained for pure $1\sigma_g$ or pure $1\sigma_u$ hole states. But since the experi-
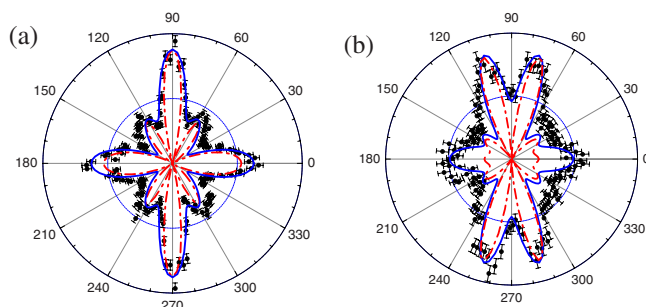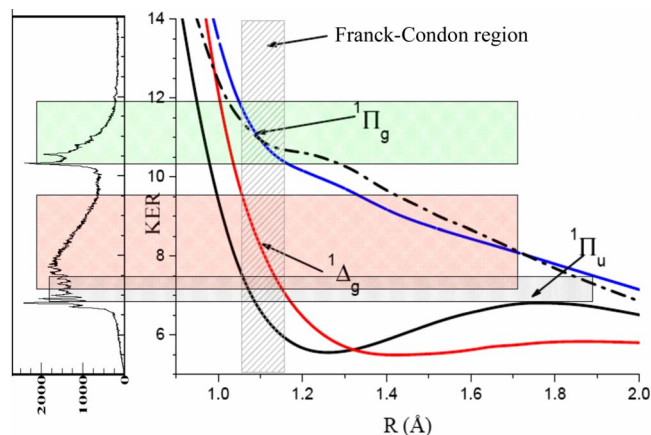

FIG. 3. (Color online) Auger-electron angular distributions (points with error bars) in arbitrary units corresponding to the decay of the $1\sigma_g$ (a) and $1\sigma_u$ (b) hole states obtained by integration of the results of Fig. 2 over KER energy from 8 to 9 eV. Molecular axis is directed along the horizontal axis. The dot-dashed and solid lines (see the text for detail) show the results of theoretical calculations (normalized to the experiment) including the Auger transitions to the doubly charged molecular ion states $(1\pi_u)^{-2}$ $^1\Delta_g$ and $(1\pi_u)^{-2}$ $^1\Sigma_g^+$.

mental separation of the $1\sigma_g$ and $1\sigma_u$ hole states is not complete, a small contribution of the state of the opposite parity is always present. Therefore the solid curves show the theoretical results including a small admixture of the hole state of the opposite parity. The amount of admixture is defined by fitting to the experiment. The theoretical curves obtained in that way correctly describe all characteristic features of the experimental angular distributions. Small remaining differences can be attributed to the neglect of the configuration interaction between doubly charged molecular ion states, as well as to the contribution of the interference between different final channels [21,22]. As it follows from the results published in [21], the configuration mixing for the main transitions contributing to the Auger spectrum here is not substantial.

By analogous study we have found that in the KER energy region between 7 and 7.5 eV three terms are giving a visible contribution, $(3\sigma_g)^{-1}$ $(1\pi_u)^{-1}$ $^1\Pi_u$, $(1\pi_u)^{-2}$ $^1\Sigma_g^+$, and $(1\pi_u)^{-2}$ $^1\Delta_g$. Finally, in the KER region between 10.5 and 11.5 eV the angular distribution is essentially defined by two terms, $(2\sigma_u)^{-1}$ $(1\pi_u)^{-1}$ $^1\Pi_g$ and $(1\pi_u)^{-2}$ $^1\Sigma_g^+$. These conclusions are in agreement with the behavior of the repulsive potential-energy curves for the $(3\sigma_g)^{-1}$ $(1\pi_u)^{-1}$ $^1\Pi_u$, $(1\pi_u)^{-2}$ $^1\Delta_g$, and $(2\sigma_u)^{-1}$ $(1\pi_u)^{-1}$ $^1\Pi_g$ states known from the literature [3,23–25]. The contributions of the corresponding triplet final states have not been revealed. According to the calculations of Ågren [21] their contributions are expected to be several times smaller.

Figure 4 shows the total KER spectrum (that is without coincidence with the photoelectrons and integrated over the angle θ) together with potential-energy curves for the most important dicationic final states. The KER spectrum contains several strong discrete lines and a continuous part. Qualitatively, this spectrum is similar to the KER spectrum observed in [3] after electron scattering. According to the results demonstrated above, a broad maximum between 7 and 10 eV is mainly formed by the transition to the $(1\pi_u)^{-2}$ $^1\Delta_g$ state. It coincides with the region where the corresponding potential-

energy curve crosses the Frank-Condon (FC) region as is shown in the figure by shaded area. In the region between 6.8 and 7.5 eV a substantial contribution is given by the transition to the $(3\sigma_g)^{-1}(1\pi_u)^{-1}\,^1\Pi_u$ final state. This is also in a good agreement with the position of the corresponding potential-energy curve inside the FC region. It is worth while to mention that due to the potential barrier at the internuclear distance of about 1.8 Å the contribution of this state has a sudden jump at KER ≈ 6.7 eV, while the contribution of the $(1\pi_u)^{-2}\,^1\Delta_g$ state is smoothly increasing and then decreasing within the FC region. Finally, the maximum between 10.3 and 11.5 eV is formed mainly by the $(2\sigma_u)^{-1}(1\pi_u)^{-1}\,^1\Pi_g$ state. There are two calculations of the potential-energy curves for this state shown in Fig. 4 which do not coincide well within the FC region. The sharp increase in the Auger-electron intensity at KER $=10.25$ eV definitely can be attributed to the presence of some potential barrier like in the case of the $^1\Pi_u$ final state, or at least to a nonmonotonic decrease in the potential-energy curve like in the calculations of Taylor [24]. But in the latter case the position of the potential-energy curve inside the FC region does not fit the position of the maximum in the experimental KER spectrum. Therefore we conclude that the potential-energy curve for the $^1\Pi_g$ dicationic state needs to be calculated more accurately.

The contribution of the $(1\pi_u)^{-2}\,^1\Sigma_g^+$ state does not produce a well separated maximum in the KER spectrum as shown in Fig. 4 though it is present in all energy region studied above as it is evident from Fig. 2 (the region of $\cos\theta = 1$ or -1). From the analysis of the Auger-electron angular distributions presented in Fig. 2 we concluded that a strong discrete transition at KER equal to 6.8 eV (see Fig. 4) belongs to the $(2\sigma_u)^{-1}(3\sigma_g)^{-1}\,^3\Sigma_u$ state. Two other strong

discrete transitions at KER $=10.32$ and 10.54 eV can be unambiguously indentified as transitions to the $(2\sigma_u)^{-1}(3\sigma_g)^{-1}$ $^1\Sigma_u^+$ state in agreement with the identification made earlier by Lundqvist *et al.* [3].

In conclusion, we have shown that the coincidence measurement of photoelectrons and Auger electrons together with the singly charged atomic ions allows separating Auger decay channels corresponding to the $1\sigma_g$ and $1\sigma_u$ hole states of N_2 without the need to separate these transitions in energy. In addition, it becomes possible to disentangle the contributions of different repulsive doubly charged molecular ion states as a function of KER energy by comparison with corresponding theoretical Auger-electron angular distributions in the molecular fixed frame. In this way one can trace experimentally the behavior of the potential-energy curves for dicationic final states inside the Frank-Condon region. To the best of our knowledge, that cannot be done by any other method. The strongest discrete lines can also be identified by this method. Evidently, this method is applicable to other homonuclear diatomic molecules.

[1] W. E. Moddeman *et al.*, J. Chem. Phys. **55**, 2317 (1971).
[2] W. Eberhardt, E. W. Plummer, I. W. Lyo, R. Carr, and W. K. Ford, Phys. Rev. Lett. **58**, 207 (1987).
[3] M. Lundqvist *et al.*, J. Phys. B **29**, 1489 (1996).
[4] T. Jahnke *et al.*, Phys. Rev. Lett. **88**, 073002 (2002).
[5] M. S. Schöffler *et al.*, Science **320**, 920 (2008).
[6] R. Dörner *et al.*, Phys. Rep. **330**, 95 (2000).
[7] J. Ullrich *et al.*, Rep. Prog. Phys. **66**, 1463 (2003).
[8] T. Jahnke *et al.*, J. Electron Spectrosc. Relat. Phenom. **141**, 229 (2004).
[9] U. Hergenhahn *et al.*, J. Phys. Chem. A **105**, 5704 (2001).
[10] S. K. Semenov *et al.*, J. Phys. B **39**, 375 (2006).
[11] M. Ehara *et al.*, J. Chem. Phys. **124**, 124311 (2006).
[12] J. L. Dehmer and D. Dill, Phys. Rev. Lett. **35**, 213 (1975).
[13] Q. Zheng, A. K. Edwards, R. M. Wood, and M. A. Mangan, Phys. Rev. A **52**, 3940 (1995).
[14] A. K. Edwards, Q. Zheng, R. M. Wood, and M. A. Mangan,

Phys. Rev. A **55**, 4269 (1997).
[15] Th. Weber *et al.*, J. Phys. B **34**, 3669 (2001).
[16] O. Jagutzki *et al.*, Nucl. Instrum. Methods Phys. Res. A **477**, 244 (2002).
[17] S. K. Semenov and N. A. Cherepkov, Phys. Rev. A **66**, 022708 (2002).
[18] S. K. Semenov *et al.*, J. Phys. B **37**, 1331 (2004).
[19] K. Zähringer, H. D. Meyer, and L. S. Cederbaum, Phys. Rev. A **45**, 318 (1992); **46**, 5643 (1992).
[20] S. K. Semenov *et al.*, Phys. Rev. A **75**, 032707 (2007).
[21] H. Ågren, J. Chem. Phys. **75**, 1267 (1981).
[22] H. Ågren, A. Cesar, and C. M. Liegener, Adv. Quantum Chem. **23**, 1 (1992).
[23] E. W. Thulstrup and A. Andersen, J. Phys. B **8**, 965 (1975).
[24] P. R. Taylor, Mol. Phys. **49**, 1297 (1983).
[25] R. W. Wetmore and R. K. Boyd, J. Phys. Chem. **90**, 5540 (1986).